

A METHOD OF MEASURING SNOW PARTICLE SIZE FROM VIDEO IMAGES FOR METEOROLOGICAL RADAR OBSERVATIONS

Masahiko HATANAKA¹, Yoshiyuki OHTA^{1,2}, Akira NISHITSUJI^{1,3},
Takeshi SAKAGUCHI¹ and Makoto WADA⁴

¹*Faculty of Engineering, Muroran Institute of Technology,
27-1, Mizumoto-cho, Muroran 050*

²*Mobile Radio Terminals Development Section, Fujitsu Hokkaido Digital Technology Ltd.,
3-1, Kita-7, Nishi-4, Kita-ku, Sapporo 060*

³*Faculty of Business Administration and Information Science,
Hokkaido Information University, 59-2, Nishinopporo, Ebetsu 069*

⁴*National Institute of Polar Research, 9-10, Kaga 1-chome, Itabashi-ku, Tokyo 173*

Abstract: For meteorological radar observations, it is very important to know the size and the characteristics of precipitation particles. In this paper, we report a method to measure snow particle size using snow particle video images. An image of snow particles, which was recorded by a specially designed portable video camera set on the ground, was digitized by a popular-priced personal computer. To reduce background offset, we used subtraction processing between images at different recording times. Using projection data on this image, the position of each snow particle was detected. Finally, we measure the three kinds of snow particle "radius". We applied this method to two sets of VCR tapes that had been recorded at Syowa Station, Antarctica, on April 5-6 and on October 1, 1988, and obtained relative distributions.

1. Introduction

A five-year program of Antarctic Climate Research (ACR) was carried out at Syowa, Asuka and Mizuho Stations, including both the interior ice sheet and sea ice area; from 1987 to 1991 by the Japanese Antarctic Research Expedition (JARE) as a part of the international cooperating World Climate Research Program (WCRP) (YAMANOUCHI and TAKEBE, 1990). In this program, a vertical pointing radar (9.41 GHz) was used to measure the amount of snowfall and the ice water content in the atmosphere continuously from 1988 to 1989 at Syowa Station (WADA, 1990). From these observed radar echo data, we have been studying a method to evaluate the precipitation rate at each altitude using microwave back scattering cross section of snow particle and normalized snow particle size distribution (HOSHIYAMA, *et al.*, 1992; TAKEYA *et al.*, 1994), in place of the radar Z factor and precipitation rate (Z-R) relation.

Recently, MURAMOTO *et al.* (1989, 1990, 1992) reported a method to measure the size and velocity of falling snowflake precisely by using video cameras, a personal computer and an image processor, and they observed snowflakes in Japan. In this paper, we report a method to observe snow particles at Syowa Station, Antarctica using a specially designed portable video camera set and to measure the size of snow particles, and show our evaluated snow particle size relative distributions.

2. Method

Snow particles on the ground were recorded by a black-and-white video camera set, as shown in Fig. 1. In this figure, the transparent film is advanced intermittently, and snow particles are accumulated on this film while it is stationary. The lights are used in night time observations. The images of accumulated snow particles on this film are recorded by a video camera and a video cassette recorder (VCR).

The video image, which is retrieved from this cassette tape, is divided into 640×480 pixels and quantized to 256 gray levels by a video digitizer in a personal computer. To recognize each snow particle, we use the following procedures:

[1] To reduce background offset level on the image and to eliminate snow particles overlapped on snow particles accumulated on the film, we use subtraction processing between images at different recording times. In case of daytime video images, the subtracted image must be sign-reversed, since daylight is obstructed by snow particles, the pixel values in snow particles are lower than the values in the background (part of the sky) and subtracted snow particle images have negative pixel values.

[2] The x -projection data, *i.e.* summations of pixel values along lines parallel to the x -axis, on this subtracted image and the y -projection data are obtained (Fig. 2a).

[3] Using a suitable threshold value in this projection data on x -axis, snow particles are separated from the background and values of the size Δx_i and the middle position x_i for each snow particle on this x -projection data are estimated. In the same manner, the size Δy_j and the middle position y_j are determined on the y projection.

[4] To confirm its position, the values of several pixels in a rectangle area (Δx_i and Δy_j), which is estimated by every combination of x_i and y_j , are checked to determine whether a particle is there or not. This processing looks like back projection processing from the x - and y -axes (Fig. 2b).

[5] Except for small rectangle images less than 50 pixels, the recognized rectangle image is cut out from the subtracted digitized image with a uniform margin (Fig. 3), and it is stored in the data base file.

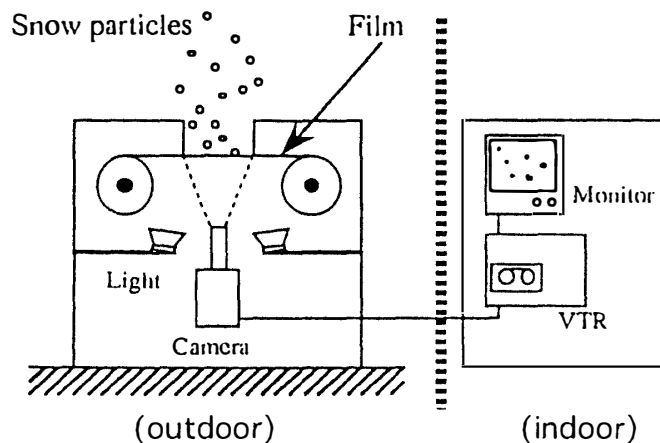


Fig. 1. Configuration of the video camera set.

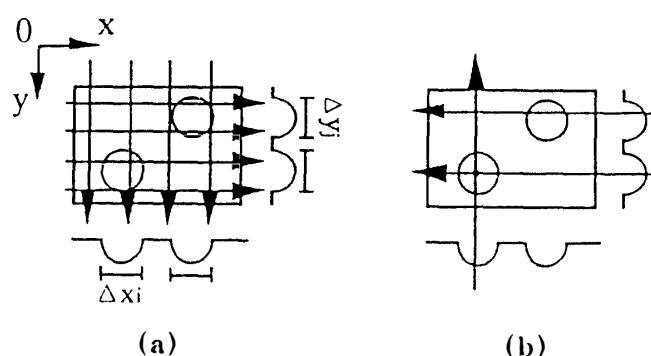


Fig. 2. Overview of (a) the projection and (b) the back projection processing on the subtracted snow particles image.

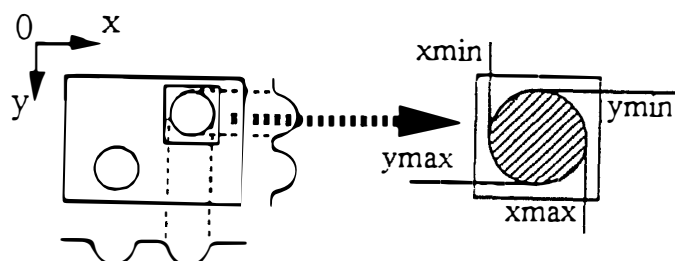


Fig. 3. Overview of the cutout processing on the subtracted snow particles image.

Since the radar cross section of snowfall is usually calculated on the assumption that snow particles are spherical (KERR, 1964), we measure three kinds of snow particle “radius” on the recognized image. The first is the maximum radius r_MAX , that is the maximum distance between the center of gravity and periphery. The second is another maximum radius r_max , which is half of the maximum distance between peripheral points through the center of gravity. The third is the equivalent radius r_area , which is calculated from the area of the particle image. To measure “radius”, we use the following procedures (ROSENFELD and KAK, 1982):

[6] To segment the recognized rectangle image into particle and background, this image was binarized (1 or 0) using the same threshold in step [3]. In this processing, if there is an unexpected pixel in the image, for example a less negative pixel value than the threshold, we ignored this image.

[7] The area and the center of gravity of this particle were computed from the total sum and x - and y -moment of pixel values in this binarized rectangle image, and the distance between two points was simply calculated by the Pythagorean theorem.

3. Equipment and Materials

The outdoor unit in Fig. 1 was specially designed to work well in low temperature environments, its dimensions and weight are 40 cm(L) * 20 cm(W) * 60 cm(H) and about 10 kg. The aperture window size is 24 mm(W) * 32 mm(L) and the transparent

film size is 35 mm(W) * 100 ft(L). The winding interval of this film is set by a variable time switch; the time wasted advancing the film is about 10 s. The indoor unit consisted of a home VCR and a monitor. For image processing, we used a popular-priced personal computer with a personal-use video digitizer board (640×400 pixels, 24 bits full color, digitizing time is 1/30 s) and a frame memory board. The final digitized pixel size is 1/30 mm. It was assumed that the gray scale level is equal to the mean of the R, G and B pixel values.

We used two sets of video cassette tape recorded at Syowa Station, Antarctica. Set a was recorded from 2113 LT on April 5 to 0133 LT on April 6 and set b was from 1800 LT to 1944 LT on October 1, 1988. In these observations, the winding interval was set for 90 s and the snow particle accumulation time was about 80 s. The meteorological conditions during these two cases are summarized in Table 1.

Table 1. Meteorological conditions for case a and b.

	Case a	Case b
Date	April 6, 1988	October 1, 1988
Mean surface air temperature	-8.1 °C	-13.5 °C
Mean surface humidity	84%	73%
Mean surface atmospheric pressure	990 mb	1000 mb
Mean wind speed	2.8 m/s	0.7 m/s

4. Results and Discussion

An example of subtraction processing (step [1]) is shown in Fig. 4. Typical subtraction intervals were 5 s for case a and 15 s for case b, respectively. Two examples of results from the projection processing to the image cutting out processing (steps [2] to [5]) are shown in Fig. 5. Since random noise and uneven offset on the subtracted background image are both positive and negative values and they tend to be canceled out on the projection data, we could use the lower threshold value ($3 = 1\%$ of 256 gray level) to obtain maximum contours of the particle. There were a few rectangle images which contained two or three particles (see Fig. 5b). To separate the snow particles in the rectangle image, we used the same steps [2] to [5] for this image, again. Four examples of measured values of the maximum radius r_{max} and the equivalent radius r_{area} with enlarged snow particle images are shown in Fig. 6. In step [5], many small particles less than 0.02 cm in radius were ignored; these particles are not important for our 9.41 GHz (wavelength 3.19 cm) meteorological radar analysis because their back scattering cross sections and reflectivities are decreasing rapidly (SKOLNIK, 1980; HATANAKA *et al.*, 1992).

More than 2500 particles were counted in case a and 1000 in case b. Particles were classified in the size ranges per 0.005 cm radius. Obtained results are shown in Fig. 7. According to the shape of the LAWS and PARSONS distribution (1943), these results can be approximated by a straight line on semi-logarithmic graph paper.

$$N(r) \sim 10^{-B*r} \quad (1)$$

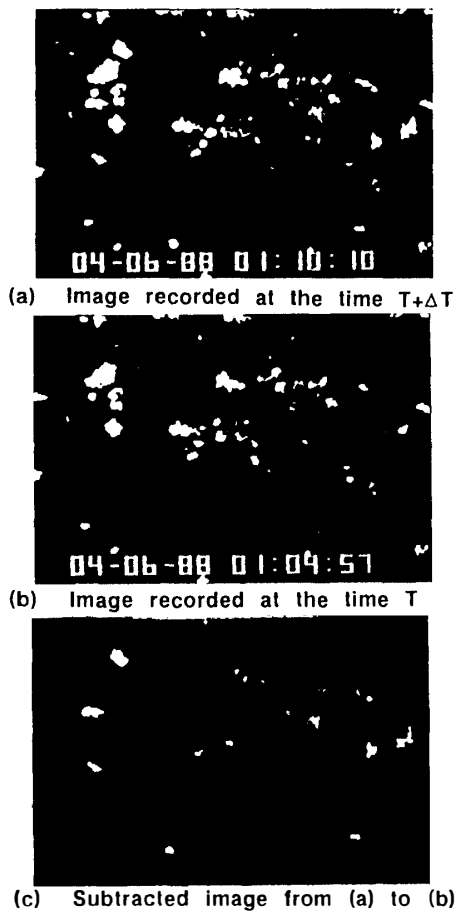


Fig. 4. A result of the image subtraction processing.

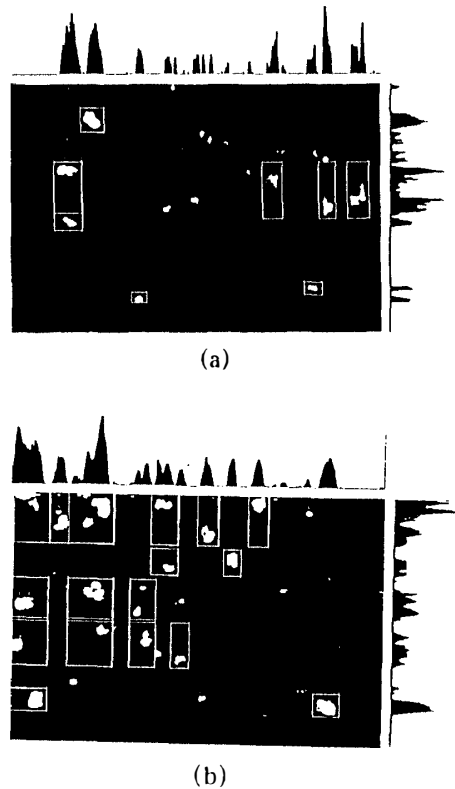


Fig. 5. Examples of the snow particles projection data and the recognized snow particles.

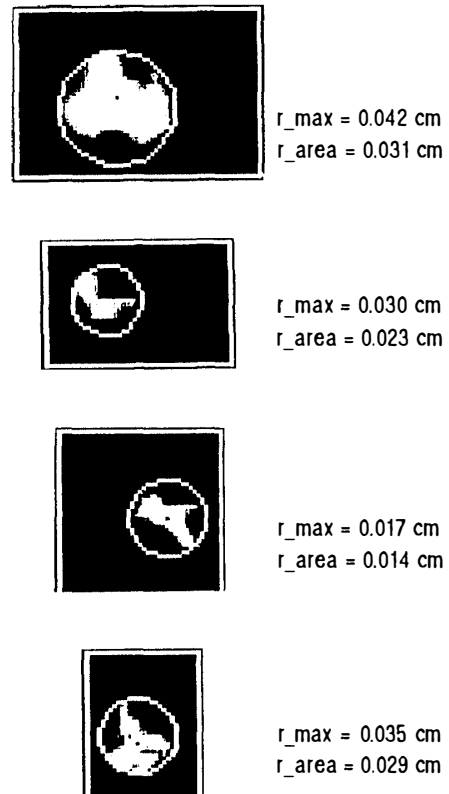


Fig. 6. Examples of the cut images and measured radii (r_{max} and r_{area}).

where r is a snow particle radius (r_{MAX} , r_{max} or r_{area}) and B is a parameter determined by curve fitting. The results of curve fitting are also shown in Fig. 7. In Fig. 7a, the snow particles, suspected graupels from the VCR image, were mainly distributed up to 0.08 cm in r_{MAX} , 0.07 cm in r_{max} , and up to 0.06 cm in r_{area} . The values of parameter B based on r_{MAX} , r_{max} and r_{area} decreased monotonously, and the B value of r_{area} was smaller than two times the r_{MAX} . Otherwise, in Fig. 7b, the snow particles, suspected aggregates of bullets, were distributed up to 0.06 cm in r_{MAX} and r_{max} , but up to 0.04 cm in r_{area} . The B value of r_{area} was larger than two times the r_{MAX} . This means that the shapes of snow particles in case b are considered to deviate more from the spherical.

We measured three kinds of “radius” (r_{MAX} , r_{max} and r_{area}). Which kind of “radius” is suitable for analysis of the radar observation data? According to our

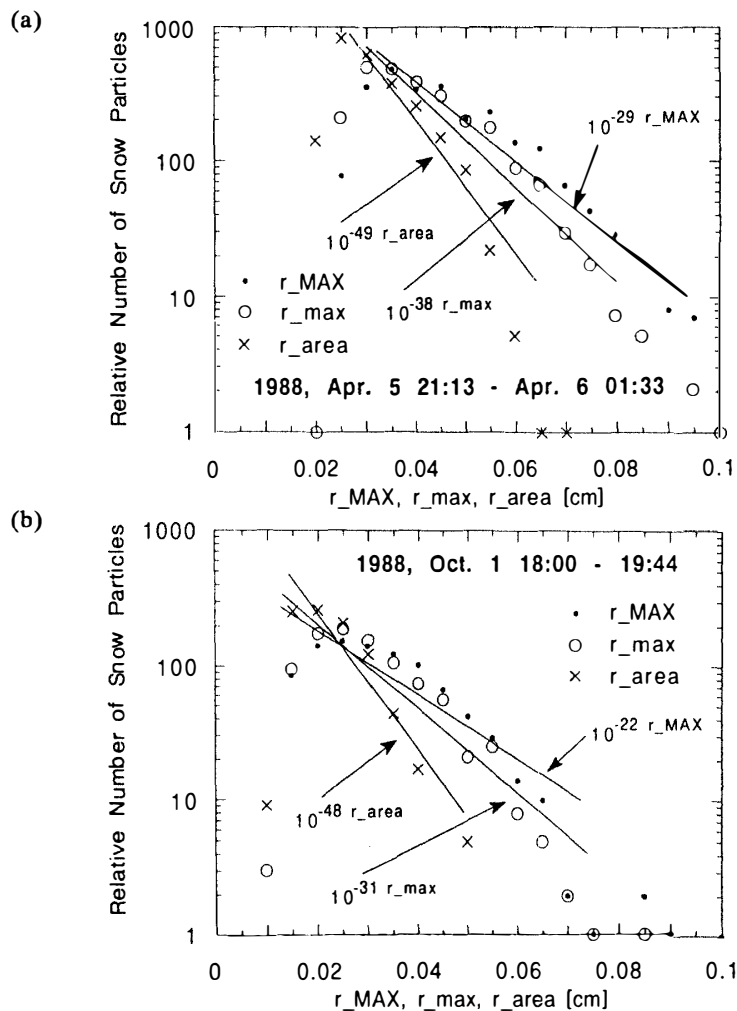


Fig. 7. Obtained snow particle size relative distributions at Syowa Station, Antarctica. (a) Case a, from 2113 LT on April 5 to 0133 LT on April 6, and (b) case b, from 1800 LT to 1944 LT on October 1, 1988.

preliminary evaluation for precipitation rates at Syowa Station using the observed meteorological radar data (TAKEYA *et al.*, 1994), our evaluated precipitation rates, which were based on the normalized snow particle maximum radius distributions N_0 (r_{\max}) obtained from Fig. 7, was compatible with the results from the measured radar Z factor and precipitation rate (Z - R) relation (KONISHI *et al.*, 1992). We think that these obtained relative distributions maintain first-order precision for our meteorological radar analysis.

Some snow particles changed their shapes and/or were fragmented on the transparent film. The procedure at step [5] removed most of these fragments, but the measured radius values of the deformed particles obviously contained error. Positions of some particles on this film during its stationary state were sometimes changed by wind, and many particles flew away from the field of view or their displacements during subtraction intervals were smaller than the typical size of the rectangle image. In these cases, since the subtracted images tend to include negative pixel values, the procedure at step [6] was useful to remove many of these rectangle images. At the current status of our meteorological radar analysis, it is difficult to say that these kinds of errors are more serious than the error caused by the assumption of spherical snow particles, *i.e.* the differences among our three kinds of "radius".

5. Conclusions

We tested a specially designed portable video camera set for obtaining snow particles at Syowa Station, Antarctica. The obtained snow particle video images were analyzed by a popular-priced personal computer with personal-use video digitizer board and frame memory board. The algorithm to measure particle size was expressed a series of well known steps. Although there are some limitations on accuracy, we obtained two sets of snow particle size relative distributions for our meteorological radar observations and their analysis.

References

- HATANAKA, M., HOSHIYAMA, M. and NISHITSUJI, A. (1992): Kishô rêdâ no atarashii kaisekihô ni yoru takasa-goto no kôsui kyôdo no suitei (2) (On the estimation of the precipitation rate at each altitude by a new analytical method for the meteorological radar echo (2)). The 15th Symposium on Polar Meteorology and Glaciology Programme and Abstracts. Tokyo, Natl Inst. Polar Res., 104–105.
- HOSHIYAMA, M., HATANAKA, M., NISHITSUJI, A. and WADA, M. (1992): On the estimation of precipitation rate by a new analytical method for the meteorological radar echo (abstract). Proc. NIPR Symp. Polar Meteorol. Glaciol., 6, 145.
- KERR, D.E. (1964): Propagation of Short Radio Waves. Lexington, Boston Technical Publ., 445–451.
- KONISHI, H., MURAMOTO, K., SHIINA, T., ENDOH, T. and KITANO, K. (1992): Z - R relation for graupels and aggregates observed at Syowa Station, Antarctica. Proc. NIPR Symp. Polar Meteorol. Glaciol., 5, 97–103.
- LAW, J.O. and PARSONS, D.A. (1943): The relation of raindrop size to intensity. Trans. Am. Geophys. Union, 24, 432–460.
- MURAMOTO, K., SHIINA, T., ENDOH, T., KONISHI, H. and KITANO, K. (1989): Measurement of snowflake size and falling velocity by image processing. Proc. NIPR Symp. Polar Meteorol. Glaciol., 2, 48–54.
- MURAMOTO, K., SHIINA, T., ENDOH, T., KONISHI, H. and KITANO, K. (1990): Measurement of falling

- attitudes of snowflakes using two video cameras. Proc. NIPR Symp. Polar Meteorol. Glaciol., **3**, 95–99.
- MURAMOTO, K., MATSUURA, K., SHIINA, T., ENDOH, T. and KONISHI, H. (1992): Measurement of falling motion of snowflakes using CCD camera. Proc. NIPR Symp. Polar Meteorol. Glaciol., **6**, 71–76.
- ROSENFELD, A. and KAK, A.C. (1982): Digital Picture Processing, 2nd ed., **2**. New York, Academic Press, 61–73, 209–210, 250–257, 286–290.
- SKOLNIK, M.I. (1980): Introduction to Radar Systems, 2nd ed. Singapore, McGraw-Hill International Editions, 498–503.
- TAKEYA, H., HATANAKA, M., SAKAGUCHI, T., NISHITSUJI, A., HOSHIYAMA, M. and WADA, M. (1994): A method to analyze the meteorological radar echo observed at Syowa Station, Antarctica. Proc. NIPR Symp. Polar Meteorol. Glaciol., **8**, 169–177.
- WADA, M. (1990): Antarctic climate research data, Part 2. Radar and microwave radiometer data at Syowa Station, Antarctica from March to December 1988. JARE Data Rep., **153** (Meteorology 24), 1–17.
- YAMANOUCHI, T. and TAKEBE, H. (1990): Report on Antarctic climate research observations by the 28th Japanese Antarctic Research Expedition (abstract). Proc. NIPR Symp. Polar Meteorol. Glaciol., **3**, 106–107.

(Received November 30, 1994; Revised manuscript received May 8, 1995)